International Journal of Nanomedicine

Dovepress
open access to scientific and medical research

Open Access Full Text Article

ORIGINAL RESEARCH

Screening of Chitosan Derivatives-Carbon Dots Based on Antibacterial Activity and Application in Anti-*Staphylococcus aureus* Biofilm

Dan Zhao[1,2], Rui Zhang[1,2], Xuemei Liu[1,2], Xiaoyun Li[1,2], Mengyu Xu[1,2], Xianju Huang[1,2], Xincai Xiao[1,2]

[1]School of Pharmaceutical Sciences, South-Central University for Nationalities, Wuhan, 430074, People's Republic of China; [2]National Demonstration Center for Experimental Ethnopharmacology Education (South-Central University for Nationalities), Wuhan, 430065, People's Republic of China

Correspondence: Dan Zhao, Tel +1 806 208 4690, Email wqzhdpai@163.com

Introduction: Pathogenic bacteria, especially the ones with highly organized, systematic aggregating bacteria biofilm, would cause great harm to human health. The development of highly efficient antibacterial and antibiofilm functional fluorescent nanomaterial would be of great significance.

Methods: This paper reports the preparation of a series of antibacterial functional carbon dots (CDs) with chitosan (CS) and its derivatives as raw materials through one-step route, and the impact of various experiment parameters upon the optical properties and the antibacterial abilities have been explored, including the structures of the raw materials, excipients, and solvents.

Results: The CDs prepared by quaternary ammonium salt of chitosan (QCS) and ethylenediamine (EDA) exhibit multiple antibacterial effects through membrane breaking, DNA and protein destroying, and the production of singlet oxygen. The CDs showed excellent broad-spectrum inhibitory activity against a variety of bacteria (Gram-positive and negative bacteria), in particular, to the biofilm of *Staphylococcus aureus* with minimum inhibitory concentration at 10 μg/mL, showing great potential in killing bacteria and biofilms. The biocompatibility experiments proved that QCS-EDA-CDs are non-toxic to human normal hepatocytes and have low haemolytic effect. Furthermore, the prepared QCS-EDA-CDs have been successfully used in bacterial and biofilm imaging thanks to their excellent optical properties.

Conclusion: This paper explored the preparation and application of functional CDs, which can be used as the visual probe and therapeutic agents in the treatment of infections caused by bacteria and biofilm.

Keywords: carbon dots, antibacterial activity, bacterial imaging, anti-biofilm, antibacterial mechanism

Introduction

The infections caused by pathogenic bacteria often cause food safety and human health problems. Besides the planktonic state, biofilm is also the most common form of bacteria, that is, the highly organized and systematic aggregation of bacteria. In recent years, various nanomaterials, such as gold nanocrystals,[1] silver nanoparticles,[2] carbon nanotubes,[3–5] mesoporous silica nanoparticles,[6,7] nanoflowers[8] and carbon dots (CDs),[9–12] have been successfully applied in antibacterial[1,8,13] and antibiofilm[2–7,14] fields.

CDs have shown great potential applications in biomedical fields, and their antibacterial ability has also arisen great interests of researchers. Normally, CDs could affect physiological functions of bacteria and finally kill them through mechanisms like oxidative stress,[9] cell membrane damage,[10] induction of gene apoptosis,[11] adsorption and encapsulation.[12] However, CDs do not show effective inhibitory ability towards biofilms regardless of their strong ability to planktonic bacteria.[15] Li and his team[16] prepared a nanosystem based on CDs, whose minimum inhibitory concentration (MIC) against *Staphylococcus aureus* (*S. aureus*) was 250 μg/mL. However, when treating biofilm, its MIC

Received: 22 November 2021
Accepted: 10 February 2022
Published: 4 March 2022

Graphical Abstract

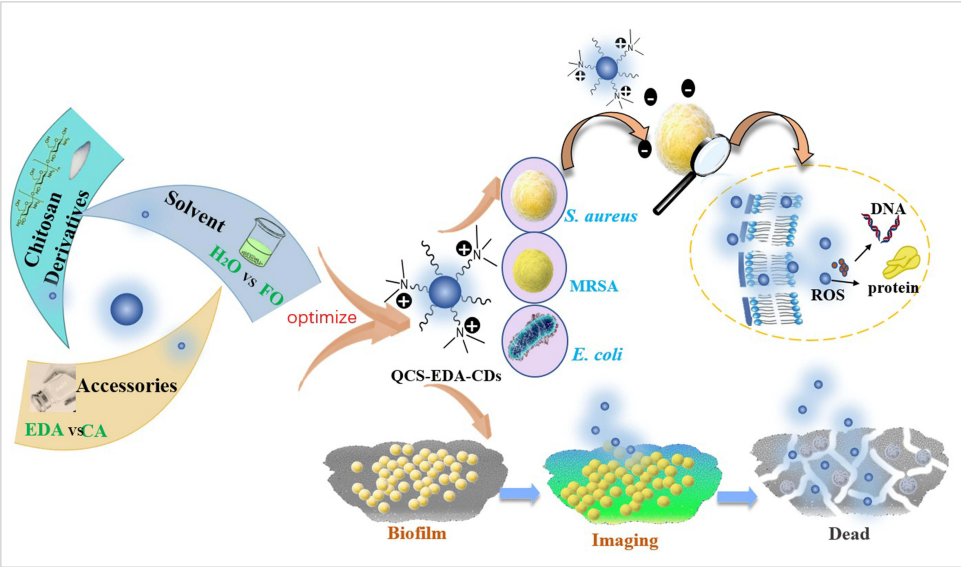

rose to 1000 μg/mL. Therefore, the development of CDs with effective ability against biofilm is of great significant to clinical application.

For the presents, CDs destroy biofilm in two ways: to kill the resident bacteria to degrade the biofilm, or to directly destroy the materials on the biofilm, such as proteins, to affect its formation. For example, Liang et al[15] used tinidazole to prepare tinidazole CDs (TCDs), and the prepared TCDs could inhibit the growth of *P. gingivalis* with MIC at 50 μg/mL and completely inhibit the formation of biofilm at 100 μg/mL. Singh and his team synthesized biomass CDs with curcumin as raw material, and CDs could interact with matrix proteins and thus possess anti-biofilm ability through biofilm degrading behavior.[17] However, reports on anti-biofilm CDs are still limited, and the antibiofilm mechanisms need further exploration.

The excellent properties of CDs are the basic requirement for their applications in antibacterial and antibiofilm field. Traditional antibacterial function of CDs was realized through coupling,[18] but the one-step route to prepare antibacterial CDs would be more attractive due to its simple operation, environmental-friendliness, low cost and stable emission.[19] It was discovered that the inhibitory behavior of prepared CDs were influenced by the types of precursors, excipients (including carbon source, nitrogen source, sulfur source, reducing agent, passivator, doping agent and acid-base regulator, etc.) and the preparation environment parameters. Analysis and filtration for raw materials, especially the ones of the same type or of the different structure domains are crucially meaningful in CDs studies. Meanwhile, the excipients and the optimization of synthesis process could also adjust the electron density and group composition, and thus the properties of the product, including the particle size and optical properties, further affecting the biochemical behavior in their practical applications. For instance, the cationic CDs could easily penetrate through or aggregate on the biofilm,[20] so chitosan (CS) with cationic group on the surface is an ideal raw material to prepare cationic antibacterial CDs.[21] Travlou et al discovered that compared with S-doped CDs, N-Doped CDs exhibited higher antibacterial ability, which was relevant to the specific surface chemical properties and particle size.[22] Huang and his team discovered that the MIC of the prepared spermidine CDs (prepared at 260 °C) against methicillin-resistant *Staphylococcus aureus* (MRSA) is at least ten times lower than that of CDs prepared at other temperatures.[23] The above researches provided meaningful basis for designing high-efficient antibacterial materials. Notably, with extraordinary optical properties and biocompatibility, CDs have also been used in microorganism monitoring.[24]

The research introduces steps to prepare blue-fluorescent CDs with chitosan (CS) and its derivatives as carbon sources through one-step hydrothermal route. The impacts of raw materials and their structures, excipients and solvents towards the antibacterial ability in prepared CDs are presented, and numerous characterization methods are adopted to study the reasons to the antibacterial behaviors of different CDs. The experiment results showed that CDs (QCS-EDA-CDs) prepared by QCS and ethylenediamine (EDA) exhibited strong inhibitory ability to several types of bacteria. Scanning electron microscope and molecular biology methods have been used to explore the impact of QCS-EDA-CDs to the growth of the bacteria. Furthermore, optical experiments showed the induced reactive oxygen species (ROS) under daylight lamp, indicating the antibacterial ability is based on multiple mechanisms. Meanwhile, CDs also exhibited strong inhibitory behavior to the biofilm of *Staphylococcus aureus* (*S. aureus*), including the formation process of biofilm and mature biofilms. The prepared the prepared QCS-EDA-CDs have low toxicity in biocompatibility evaluation, which making them ideal material as multi-colored fluorescent probe to *S. aureus* cells and biofilm imaging.

Materials and Methods

Materials

Chitosan (CS, degree of deacetylation≥95%) was obtained from Shanghai Macklin Biochemical Co., Ltd. Carboxymethyl chitosan (CMCS, degree of carboxylation≥80%), chitosan quaternary ammonium salt (QCS, degree of substitution:90%) and tryptone soy broth (TSB) were provided by Shanghai Yuanye Biological Technology Co., Ltd. Citric acid monohydrate (CA) and ethylenediamine (EDA) were provided by Sinopharm Chemical Reagent Co., Ltd. They were all AR (unless otherwise stated). Singlet oxygen sensor green reagent (SOSG) was provided by Dalian Meilun Biotechnology Co., Ltd. *Staphylococcus aureus* (*S. aureus*, CCTCC AB 91093), *Escherichia coli* (*E. coli*, CCTCC AB 93154), Methicillin-resistant *Staphylococcus aureus* (MRSA, CCTCC AB 2015107) were provided by China Center for Type Culture Collection (CCTCC).

Material Characterizations

Fluorescence spectra were measured by LS55 fluorescence spectrophotometer (PerkinElmer). Absorption spectra of Ultraviolet-visible (UV-Vis) were recorded using Lambda-35 UV-vis spectrophotometer (PerkinElmer). The transmission electron microscopy (TEM) and high-resolution TEM (HRTEM) images were analyzed using JEM-1400Plus transmission electron microscope (Japan Electron Optics Laboratory Co., Ltd). Zeta potentials for CDs were evaluated by zetasizer (Nano ZSE, Malvern Instruments, UK). VG Multilab 2000 X-ray photoelectron spectroscopy was gathered by surface analysis. Optical density (OD) in the cell was calculated using microplate reader (Thermo Scientific, England, UK). The circular dichroism spectra were gathered using Chirascan Plus spectropolarimeter (Applied Photophysics Ltd.). Scanning electron microscope (SEM) images for bacteria were conducted using Zeiss SIGMA scanning electron microscope (Carl Zeiss Jena). Fluorescence optical microscope (Nikon ECLIPSE Ti) was applied on images through laser-scanning confocal fluorescence.

Synthesis Method of CDs

The synthesis procedure of QCS-EDA-CDs was as follows: 200 mg of QCS was dissolved in 200 μL EDA and 20 mL DI water and the mixture was afterwards moved to Teflon-lined stainless-steel autoclave and preserved at 200 °C in 4 h. Synthesis methods of other CDs are in the Supplementary Materials.

Confocal Microscopic Imaging of Biofilm

S. aureus was considered a representative target bacterium. S. aureus cells were incubated in the TSB medium at 37 °C in 48 h to obtain mature biofilms. The biofilm rinsed twice in a PBS (pH = 7.4) solution for suspension removal, and suspended in 750 μL PBS solution. Finally, QCS-EDA-CDs solution was introduced into PBS solutions (Final concentrations were 250 and 500 μg/mL, respectively) with S. aureus biofilm and incubated in 2.5 h. Eventually, the biofilm and cells were investigated under confocal fluorescence microscopy.

Inhibition of Biofilm Experiments

Fresh *S. aureus* culture (10^9 CFU mL^{-1}) was diluted 1:10 in 200 μL TSB medium, which contained QCS-EDA-CDs at varying concentrations (5, 10, 15, 20, 25, 30, 40 μg/mL) on 96-well plates. Wells with no QCS-EDA-CDs were used for control. The mixture was cultured at 37°C. The OD value of per well was measured using the microplate reader at 600 nm within 48 hours. The time curve of OD_{600} at different concentrations was drawn.

Live/Dead Cell Imaging

To evaluate the inhibitory effect of the sample on the formation of biofilms, fluorescence photography was performed using the confocal laser scanning microscope (CLSM). Upon incubation, the *S. aureus* biofilm was rinsed thrice in PBS (pH = 7.4). It could be detected on CLSM after staining with DAPI/PI (10 μg/mL) for 15 minutes. The fluorescence image was obtained when the sample was simultaneously excited with 350 and 533 nm, and the corresponding emission was at 461 and 615 nm, showing blue and red, respectively.

SOSG Oxidation in the Presence of $^1O_2$

The reaction between SOSG and SOG produced from photoirradiation for QCS-EDA-CDs (1 mg/mL) in PBS was investigated. SOSG was added with a concentration of 2.5 μM. The control groups include: (1) Pure SOSG; (2) pure CDs. The tested solutions were irradiated with daylight lamp or placed in the dark for 30 minutes. The SOG was generated from irradiation at 671 nm. The SOSG fluorescence was recorded under the excitation at 494 nm, and the maximum was detected upon irradiation to decide sample SOG. Sample SOG was assessed through SOSG fluorescence enhancement in comparison with the background or control sample.[25]

Results and Discussion

The Impact of Different Conditions Upon the Antibacterial Ability of CDs

The Effects of Raw Material Type on CDs

CS and its derivatives (carboxymethyl chitosan (CMCs) and oligochitosan quaternary ammonium salt (QCS)) have been used to prepare CDs, to study the impact of carbon source domain to the inhibitory abilities of prepared products. CS-CDs, QCS-CDs and CMCS-CDs have been prepared through one-step hydrothermal route (200 °C, 4 h) (Scheme 1) with CS, CMCS and QCS as raw materials respectively. Since CS is slightly soluble in water, 1% acetic acid was used as the solvent when CS used as raw material.

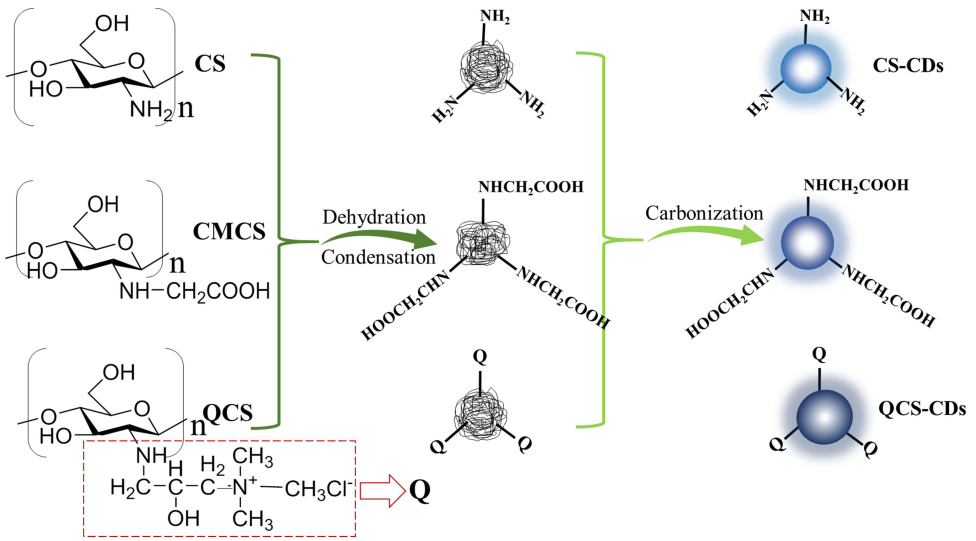

Scheme 1 CS-CDs, CMCS-CDs and QCS-CDs were prepared from CS, CMCS and QCS, respectively.

Table 1 The Emission Wavelength and Minimum Inhibitory Concentration (MIC) Against *S. Aureus* of CDs Prepared from Different Raw Materials

Types of CDs	Raw material	Solvent	MIC(μg/mL) (*S. aureus*)
CS-CDs	CS	1% Acetic acid	250
CMCS-CDs	CMCS	Water	>1000
QCS-CDs	QCS	Water	10
QCS-CA-CDs	QCS+CA	Water	125
QCS-EDA-CDs	QCS+EDA	Water	10
QCS- FO-CDs	QCS	Water+ Formamide	>1000

Figure S1 shows the UV-Vis absorption spectra and fluorescence spectra for CS-CDs, CMCS-CDs and QCS-CDs. Under abundant daylight, the CS-CDs and QCS-CDs solutions are pale yellow, and CMCS-CDs solution is brown. Their UV-vis absorption peaks are at 286, 257 and 257 nm, and all exhibit blue fluorescence under light (365 nm).

The antibacterial abilities of three prepared CDs against *S. aureus* are studied to explore the impacts of raw material structure to the antibacterial abilities of the products. According to Table 1, the minimum inhibitory concentrations (MIC) of CS-CDs, CMCS-CDs and QCS-CDs against *S. aureus* are 250, >1000 and 10 μg/mL. CMCS-CDs show almost no antibacterial ability to *S. aureus*, while QCS-CDs have the best antibacterial ability.

Scheme 1 shows the structural domain differences of CS and its derivatives. The CMCS and QCS are prepared by using carboxymethyl and 2,3-epoxypropyl trimethylammonium chloride to replace the hydrogen atom in amino group of CS. Some residual groups of these three raw materials still exist on the surface of prepared products after high temperature, dehydration, nucleation and carbonization. Since antibacterial abilities of the raw materials might be inherited into their products, the electrical properties of these three raw materials and their products are investigated to explore the reasons to the difference in antibacterial abilities (Figure S2). The MICs of CS and QCS against *S. aureus* are both 25 μg/mL, while CMCS almost does not have any antibacterial ability. The experiment results show that CMCS and its product CMCS-CDs are both negatively charged, which would prevent their interactions with negative-charged bacteria. The positive charge of CS and QCS (zeta potentials: +65.8 and +59.1 mV) and their products CS-CDs and QCS-CDs (zeta potentials: +32.9 and +30.7 mV) promises their interactions with bacteria, penetrating cell membrane and finally killing the bacteria. Since QCS-CDs exhibit better water solubility and stronger antibacterial ability than other prepared CDs, it is thus chosen as the target of further studies.

The Influence of Excipients on the Synthesis of CDs

As is known that besides carbon source, other synthesis parameters, including the nitrogen source, sulfur source, reducing agent, passivator, doping agent and acid-base regulator, could also influence the prepared CDs' optical properties, but their influences upon the antibacterial behaviors of the products are often neglected.[26]

The impacts of common auxiliary materials CA (50 mg) and ethylenediamine (EDA, 200 μL) upon the prepared QCS-CDs' properties are investigated. According to Figure 1A and B, UV-vis absorption peaks in QCS-CA-CDs and QCS-EDA-CDs are at 270 nm and 304 nm, attributed to the electron transition from σ and π orbits (occupying the highest molecule). At the excitation wavelength of 370 nm, their emission wavelengths reach 465 nm and 466 nm, almost the same as that of QCS-CDs (467 nm), showing that their luminescent groups are mainly from the carbon source QCS. Moreover, the QYs of QCS-EDA-CDs is calculated as 9.0% with quinine sulfate as reference, higher than that of QCS-CDs prepared with water as solvent (QYs=0.9%). The high fluorescence QY of EDA-passivated CDs may be attributed to the interplay between the holes trapped and the passivation of the CDs.[27] According to Table 1, the MIC in QCS-CA-CDS against *S. aureus* is 125 μg/mL, much lower than that of QCS-CDs (10 μg/mL), while the MIC of QCS-EDA-CDs is 10 μg/mL, similar to that of QCS-CDs.

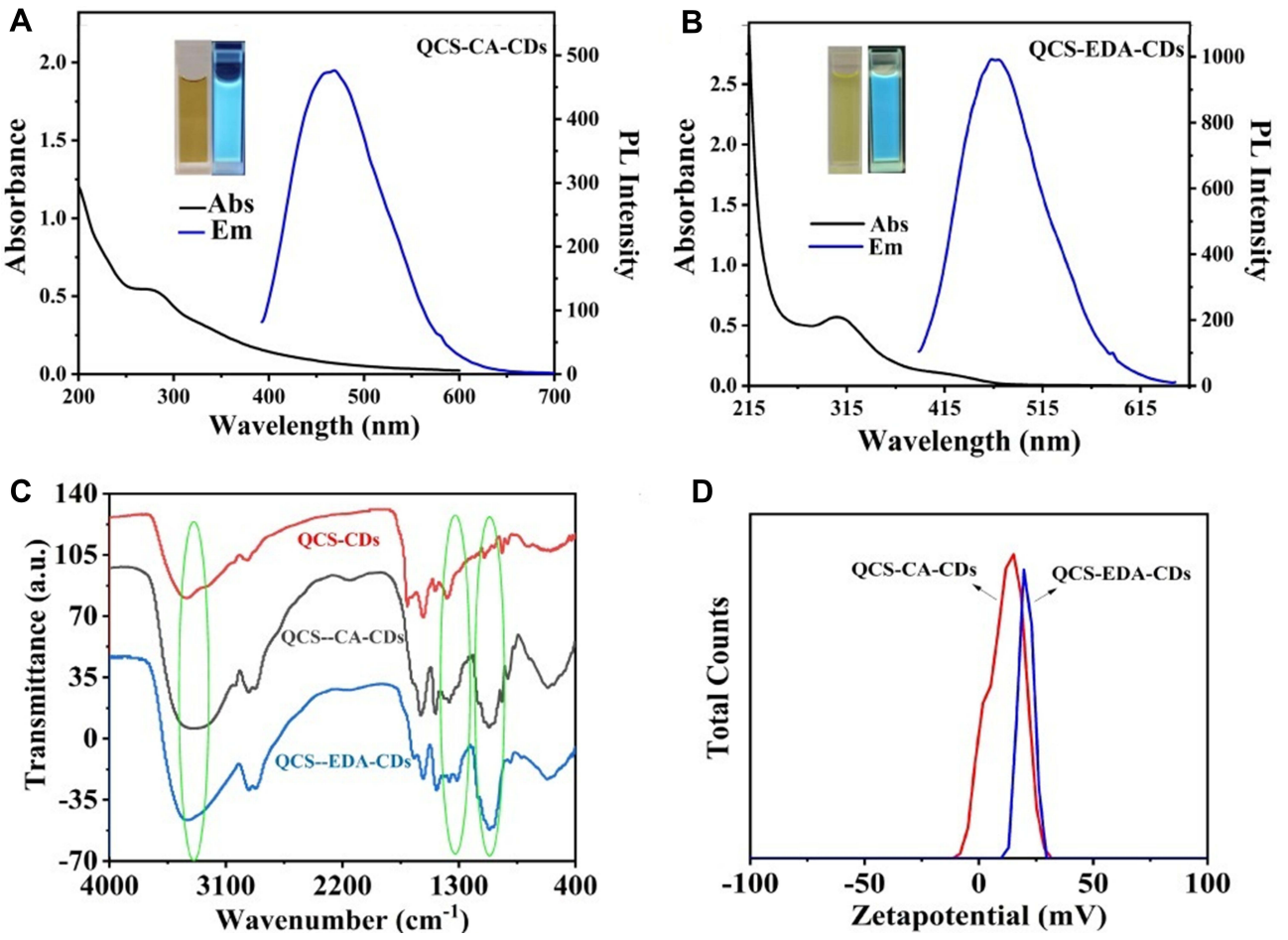

Figure 1 (**A**) The UV-Vis absorption and fluorescence spectrum for QCS-CA-CDs. Insets: QCS-CA-CDs solutions in daylight (left) and 365 nm UV lamp (right). (**B**) The UV-Vis absorption and fluorescence spectrum of QCS-EDA-CDs. Insets: QCS-EDA-CDs solutions in daylight (left) and 365 nm UV lamp (right). (**C**) FTIR spectra of QCS-CDs, QCS-CA-CDs and QCS-EDA-CDs. (**D**) zeta potential curves obtained for water suspensions of QCS-CA-CDs and QCS-EDA-CDs.

Several characterization means have been employed to compare their functional groups of these CDs to study their antibacterial mechanisms. As shown in FTIR spectra (Figure 1C), the peak of QCS-CA-CDs at 1375 cm^{-1} in infrared absorption spectra results from the in-plane bending in -OH bonds, while the peak of QCS-EDA-CDs at 1063 cm^{-1} is attributed to the vibrations of C–O bonds.[28] Besides the absorption peak of $-N^{+}(CH_3)_3$ (1488 cm^{-1}), QCS-CA-CDs also have absorption peaks of −COOH at 3398 and 1697 cm^{-1}.[29] The measured zeta potentials of these two CDs exhibit obvious difference. The zeta potential of QCS-CA-CDs is +11.7 mV (Figure 1D), lower than that of QCS-EDA-CDs (+20.6 mV). When CA is used as carbon source in preparation, the carboxyl group in the structure of CA can react with quaternary ammonium group in QCS, leading to reduced zeta potential. The changed surface group and reduced zeta potential would decrease the binding ability of prepared CDs with negatively charged bacteria, and thus its antibacterial abilities.

The Impact of Solvent Upon the Antibacterial Ability of CDs

Though the reaction solvent has been regarded as the crucial synthesis parameter for optical properties of prepared products,[30,31] the impact of solvent upon the antibacterial ability of prepared CDs still needs detailed research. Water and organic solvent FO are used as solvent to prepare QCS-CDs and QCS-FO-CDs. As shown in Figure S3a, the absorption peak of QCS-FO-CDs in UV-vis absorption spectrum reaches 271 nm, and emission wavelength reaches 449 nm at the excitation wavelength of 370 nm, shorter than the emission peak of QCS-CDs.

With *S. aureus* as target bacteria, QCS-FO-CDs exhibit almost no antibacterial ability against bacteria (MIC>1000 μg/mL), much weaker than QCS-CDs prepared in water. The enhancement of other functional groups in CD skeleton,

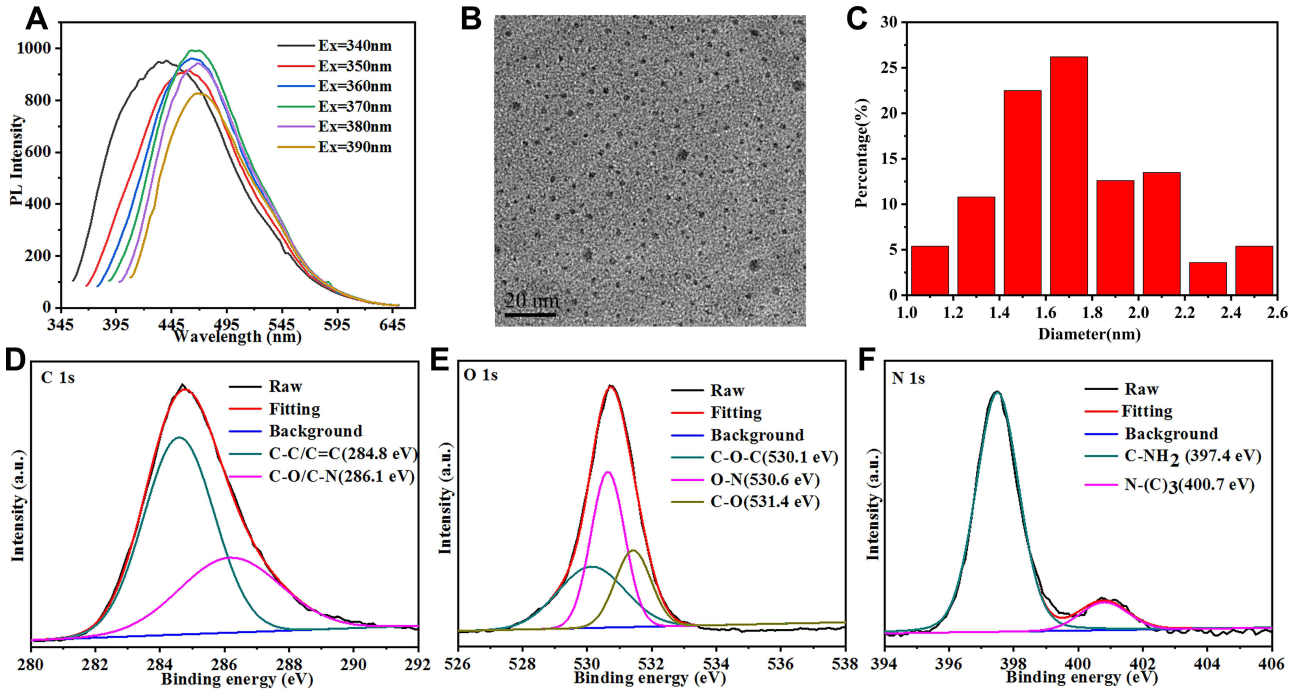

Figure 2 (**A**) Emission spectra of QCS-EDA-CDs with different excitation wavelengths. (**B**) TEM image of QCS-EDA-CDs. (**C**). Size distribution histogram of QCS-EDA-CDs. High-resolution XPS spectra (**D**) C1s, (**E**) O1s, and (**F**) N1s of QCS-EDA-CDs.

such as C=N (1630 cm^{-1}), after FO's participation in preparation process, causes zeta potential of QCS-FO-CDs to reduce to +23.2 mV (Figure S3b), much lower than that of QCS-CDs, showing the adjustment effect of the polarity of solvent during the synthesis process.

Characterization of QCS-EDA-CDs

Several characterization methods are adopted to investigate QCS-EDA-CDs' properties. The emission wavelength of QCS-EDA-CDs increases from 340 nm to 390 nm as corresponding excitation wavelength increases gradually from 439 nm to 468 nm (Figure 2A), showing its excitation wavelength dependent property. The morphology of prepared QCS-EDA-CDs is presented with TEM. According to Figure 2B and C, QCS-EDA-CDs are well-distributed and uniform in size with a narrow distribution range of 1.03–2.63 nm and their average size is about 1.74 nm. Elemental composition and chemical bonding in QCS-EDA-CDs are further investigated by XPS measurements. The high-resolution C 1s spectrum for QCS-EDA-CDs (Figure 2D) shows four peaks at 284.8 and 286.1 eV, ascribed to C=C/C–C and C–O/C–N groups.[32] The O 1s spectrum for QCS-EDA-CDs (Figure 2E) reveals two relative oxygen species of C–O–C (530.1 eV), N–O (530.6 eV) and C-O-H (531.4 eV). Three typical peaks at 397.4 and 400.7 eV in deconvoluted N 1s XPS spectrum of QCS-EDA-CDs (Figure 2F) are attributed to C-NH_2 and N–(C) $_3$ groups, respectively.[33,34]

Antibacterial Properties of QCS-EDA-CDs

Multiple experiments have been conducted to examine antibacterial abilities of QCS-EDA-CDs through broth dilution method, including its abilities against Gram-positive (*S. aureus*), Gram-negative (*E. coli*), and drug-resistant (MRSA) bacteria.

As shown in Table 2, QCS-EDA-CDs display better antibiotic impact on Gram-positive (*S. aureus*) than on Gram-negative (*E. coli*) bacteria, with MIC at 10 μg/mL against *S. aureus* and 50 μg/mL against *E. coli*. Since MRSA-caused infection of clinical treatment is always considered a difficult point of medical study, it is chosen as the sample for resistant bacteria. QCS-EDA-CDs also display extraordinary antibacterial efficiency for drug-resistant bacteria (MRSA) with MIC at 10 μg/mL. The concentration- and time-dependent bactericidal impacts of QCS-EDA-CDs on *S. aureus* can

Table 2 Antibacterial Activities of QCS-CDs Were Compared with Various Chemically Prepared NPs and CDs

Raw material	Method of preparation	Samples	Particle size (nm)	Antibacterial type	MIC (μg / mL)	Ref.
QCS, EDA	One-step hydrothermal method	QCS-EDA-CDs	1.74 (TEM)	*S. aureus*, MRSA (G^+) *E. coli* (G^-)	10 10 50	
CS, [a]TPP	Ionic gelation method	CH NPs	217 (DLS)	*S. aureus* *E. coli*	500–1000 500–1000	[35]
Eugenol modified CS, TPP	Ionic gelation method	CHCA NPs	260 (DLS)	*S. aureus* *E. coli*	500-1000 500-1000	[35]
Carvacrol modified CS, TPP	Ionic gelation method	CHEU NPs	235 (DLS)	*S. aureus* *E. coli*	500 250–500	[35]
[b]DDA, [c]GTA	One-step hydrothermal method	QCQD	5 (TEM) 3.4–4.5 (DLS)	*S. aureus* MRSA	10 10	[36]
[d]AEEA, BS-12, [e]EDC·HCl, [f]Sulfo-NHS	Two-step hydrothermal method	CDs-C_{12}	4 (TEM) 8 (DLS)	*S. aureus* *E. coli*	8 >200	[37]

Abbreviations: [a]TPP, Sodium tripolyphosphate; [b]DDA, Diallyldimethylammonium chloride; [c]GTA, 2.3-epoxypropyltrimethylammonium chloride; [d]AEEA, 3-[2-(2-aminoethylamino)ethylamino]propyl-trimethoxysilane; [e]EDC·HCl, 1-(3-(dimethylamino)propyl)-3-ethylcar bodiimide hydrochloride; [f]Sulfo-NHS, N-hydroxysulfosuccinimide.

be seen from Figure S4. At concentration of 10 μg/mL, bacterial growth is entirely prohibited by QCS-EDA-CDs at 30 h, showing QCS-EDA-CDs' long-term inhibitory ability against the bacteria.

The prepared QCS-EDA-CDs have been compared with other chitosan-derived nanoparticles and quaternized CDs reported in other references, in aspects of preparation methods and antibacterial properties (Table 2). QCS-EDA-CDs show much better antibacterial behavior against *S. aureus* than chitosan nanoparticles (CS NPs), carvacrol-grafted chitosan nanoparticles (CSCA NPs) and eugenol-grafted chitosan nanoparticles (CSEU NPs) whose MICs against *S. aureus* are beyond 500 μg/mL.[35] Though the MIC of QCS-EDA-CDs is quite close to that of quaternized CDs, QCS-CDs reported in this paper require simpler and easier synthesis process.

Since Gram-negative bacteria are in an outer membrane structure that can be hardly penetrated and protect bacteria from the antibiotics, the infection caused by Gram-negative bacteria is harder to be cured than that caused by Gram-positive bacteria. The above-mentioned references also reported the antibacterial ability of chitosan nanoparticles (CS NPs, CSCA NPs and CSEU NPs) against *E. coli*,[35] with their MIC at 0.5–1, 0.5–1 and 0.25–0.5 mg/mL respectively. QCS-EDA-CDs exhibit similar inhibitory ability as those reported nanoparticles.

The structural difference of these two types of bacteria might be the reason to such difference in exhibited antibacterial abilities of QCS-CDs. It is found that Gram-positive bacteria show greater sensitivity towards lipophilic molecules compared with Gram-negative bacteria. The cell wall of Gram-positive bacteria (such as *S. aureus*) and Gram-negative bacteria (such as *E. coli*) is in different chemical composition.[38] *S. aureus* and the corresponding bacteria have porous cell wall because of cross-linked peptidoglycan's distributed thick layer on the plasma membrane, which may promote QCS-EDA-CDs' interaction with *S. aureus* and MRSA, and thus encourage the antibacterial behavior of CDs.[39] However, the cell wall of *E. coli* contains an outer membrane and intermittently peptidoglycan network, hindering the interaction between CDs and *E. coli* and making the bacteria exhibited stronger resistance against the inhibitory behavior of CDs.

Inhibitory Abilities of QCS-EDA-CDs Against Biofilm

The inhibitory ability of prepared QCS-EDA-CDs against the bacterial biofilm is tested with pathogen *S. aureus* as the target bacteria. Compared with control group, QCS-EDA-CDs can significantly decrease biofilm amount in *S. aureus* (Figure 3), and the inhibition rate against biofilm is positively related to every antibacterial agent's concentration. When

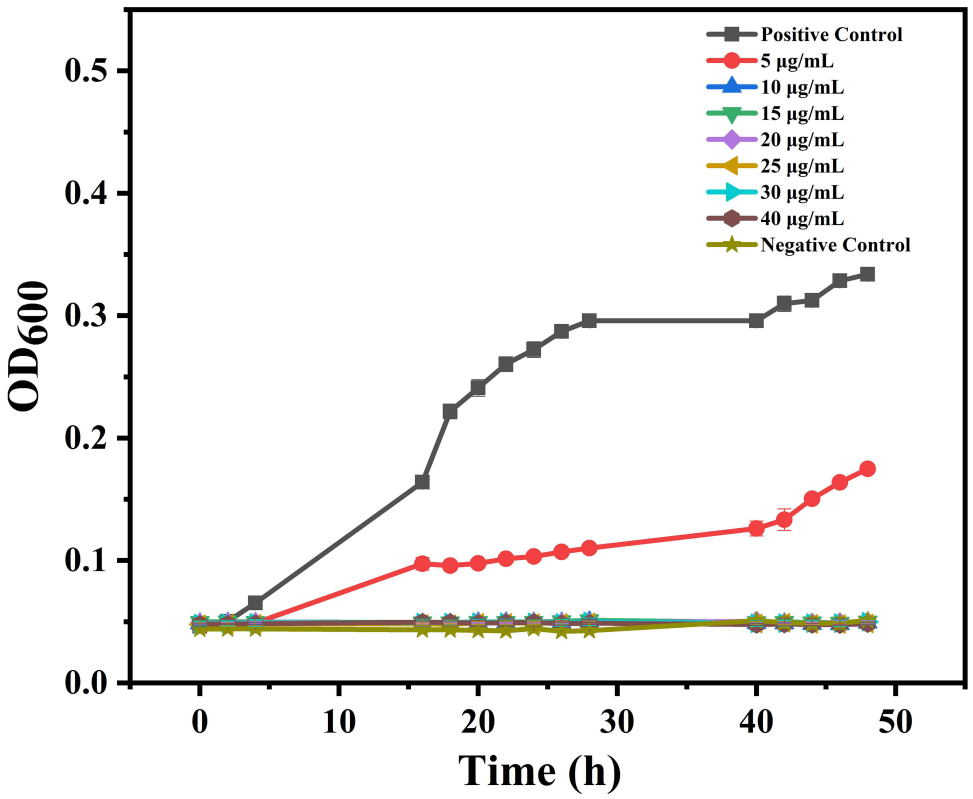

Figure 3 Inhibition effect of different QCS-EDA-CDs concentrations on *S. aureus* growth as a function of incubation time.

the concentration is above 10 μg/mL, QCS-EDA-CDs can almost completely inhibit the formation of biofilm of *S. aureus*, that is, the minimum biofilm inhibitory concentration (MBIC) is 10 μg/mL.

Table 3 Anti-Bacterial Biofilm Activities of Different Nanoparticles

Nanoparticles	Particle Size (nm)	Zeta Potential (mV)	Types of Biofilms	MIC (μg/mL)	MBIC (μg/mL)	Ref.
CDs	1.5–2.5	−15.1	*S. aureus* *P. aeruginosa*	375 500	375 500	[40]
[a]PPD@CDLys	135 (7.4) 27.3 (5.5)	+1.4 (7.4) +15.9 (5.5)	*S. aureus*	250(pH=7.4) 8(pH=5.5)	1000	[16]
[b]CDs-LP	3	−22	*E. coli*	-	800	[41]
[c]TCD	16.5	-	*P. gingivalis*	25	150	[15]
[d]Si-QAC	3.3	+33.1	*S. aureus*	50	1000	[42]
CDs	5.53	~+16 (7.4) ~+21 (5.5)	*S. aureus*	4.8 (pH=7.4) 1.2 (pH=5.5)	500	[43]
[e]CD-Gu$^+$-AmB	-	−19.16	*Candida* A. SC5314 B. ATCC 90028	A.15.63 B. 7.81	A. 31.25 B. 31.25	[44]
QCS-EDA-CDs	1.74	+20.6	*S. aureus*	10	10	

Abbreviations: [a]PPD, Poly(ethylene glycol-COOH-polyethylenimine-2,3-dimethylmaleic anhydride; [b]LP, Lactobacillus plantarum; [c]TCDs, Tinidazole; [d]QAC, Dimethyloctadecyl[3-(trimethoxysilyl) propyl] ammonium chloride; [e]CD-Gu$^+$-AmB, Guanylated carbon dots with amphotericin B-conjugation.

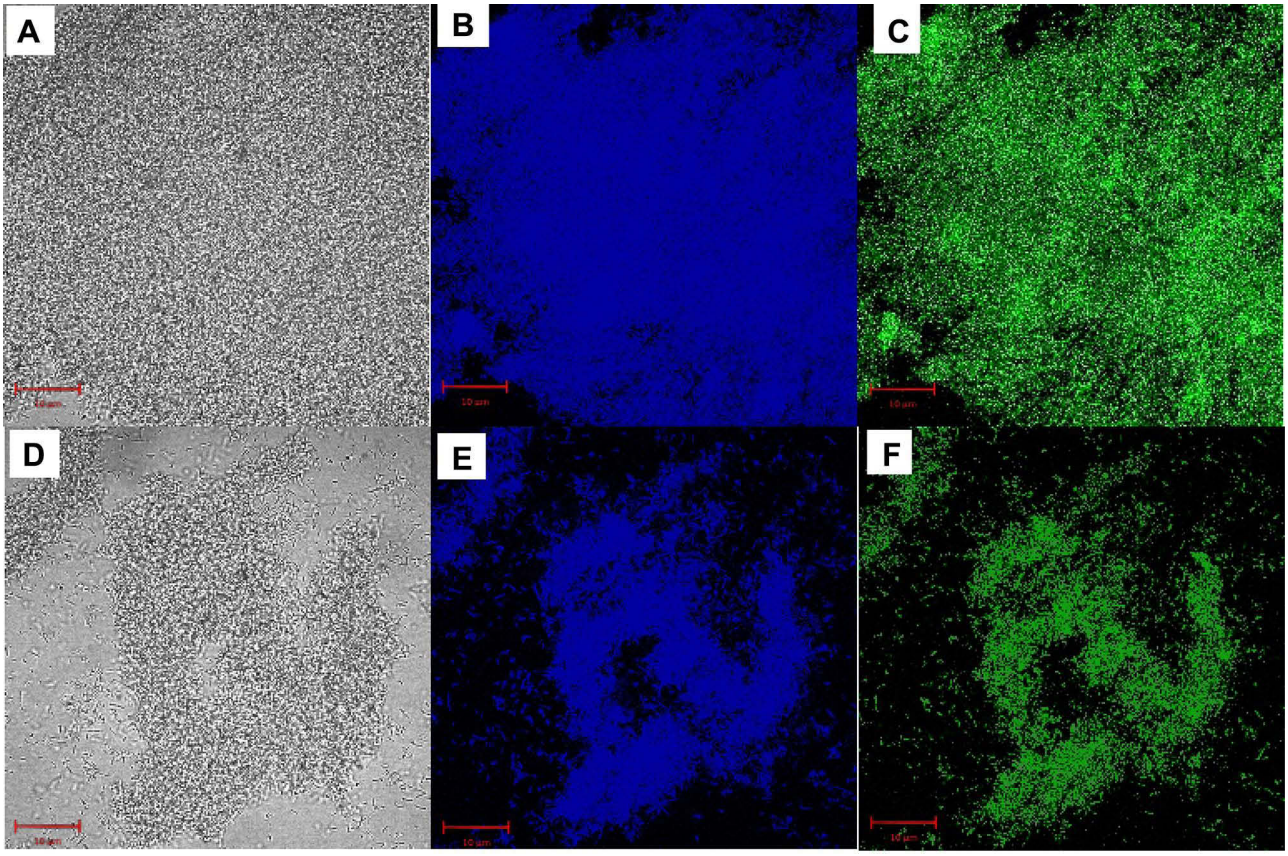

Figure 4 Fluorescence microscopy images for *S. aureus* biofilms stained by (**A-C**) 250 μg/mL and (**D-F**) 500 μg/mL QCS-EDA-CDs for 2.5 h.

Nowadays, some antibacterial nanoparticles with the activity of inhibiting biofilm have been developed.[16,40–45] However, they often have some defects, such as too large antibacterial MIC or inhibiting biofilm in a much larger amount than MIC in a short period of time, which is not conducive to the application of antibacterial materials in actual medical treatment. With reference to previous studies (such as Table 3), QCS-EDA-CDs have long-term biofilm inhibition activity, and their MBIC and MIC are not much different. This shows the superiority of QCS-EDA-CDs in inhibiting biofilms.

Recent researchers have discovered the negative activity of chitosan towards the formation of biofilm of a variety of bacteria and fungi.[45] Chitosan can inhibit the formation of biofilm, and lead to the dispersion of pre-formed biofilm. The confocal laser scanning microscope (CLSM) images of Figure 4 further show the impact of QCS-EDA-CDs upon the formation of the biofilm of *S. aureus*. Under the low concentration of QCS-EDA-CDs (250 μg/mL) (Figure 4), the biofilm shows compact structure and the internal bacterial cells are well clustered, whereas under high concentration of QCS-EDA-CDs environment, the density of biofilm has significant decrease and the bacterial debris can be obviously found. The images prove the inhibitory effects to the growth and reproduction of biofilm, as well as to the mature biofilm.

To get more directly assessment of the impact of QCS-EDA-CDs upon the mature biofilm of *S. aureus*, CLSM is also used to observe the PI/DAPI-labeled biofilms of *S. aureus* treated by QCS-EDA-CDs at different concentrations. DAPI and PI are common staining agents for live and dead cells. The wall/membrane-damaged bacteria would be dyed as red-colored, and the wall/membrane intact bacteria cells as blue-colored. As shown in Figure 5A-C, the untreated biofilm of *S. aureus* exhibits blue fluorescence without any red fluorescence. In contrast, after the treatment of QCS-EDA-CDs, the biofilm shows strong red fluorescence, illustrating the death of large amount of bacteria. Meanwhile, the biofilm treated by two concentrations of QCDs-EDA-CDs for the same duration of time (Figure 5) shows the gradual increase red fluorescence, and under the light field, the dense biofilm structure can be observed being destroyed. The result shows that the high concentration of QCS-

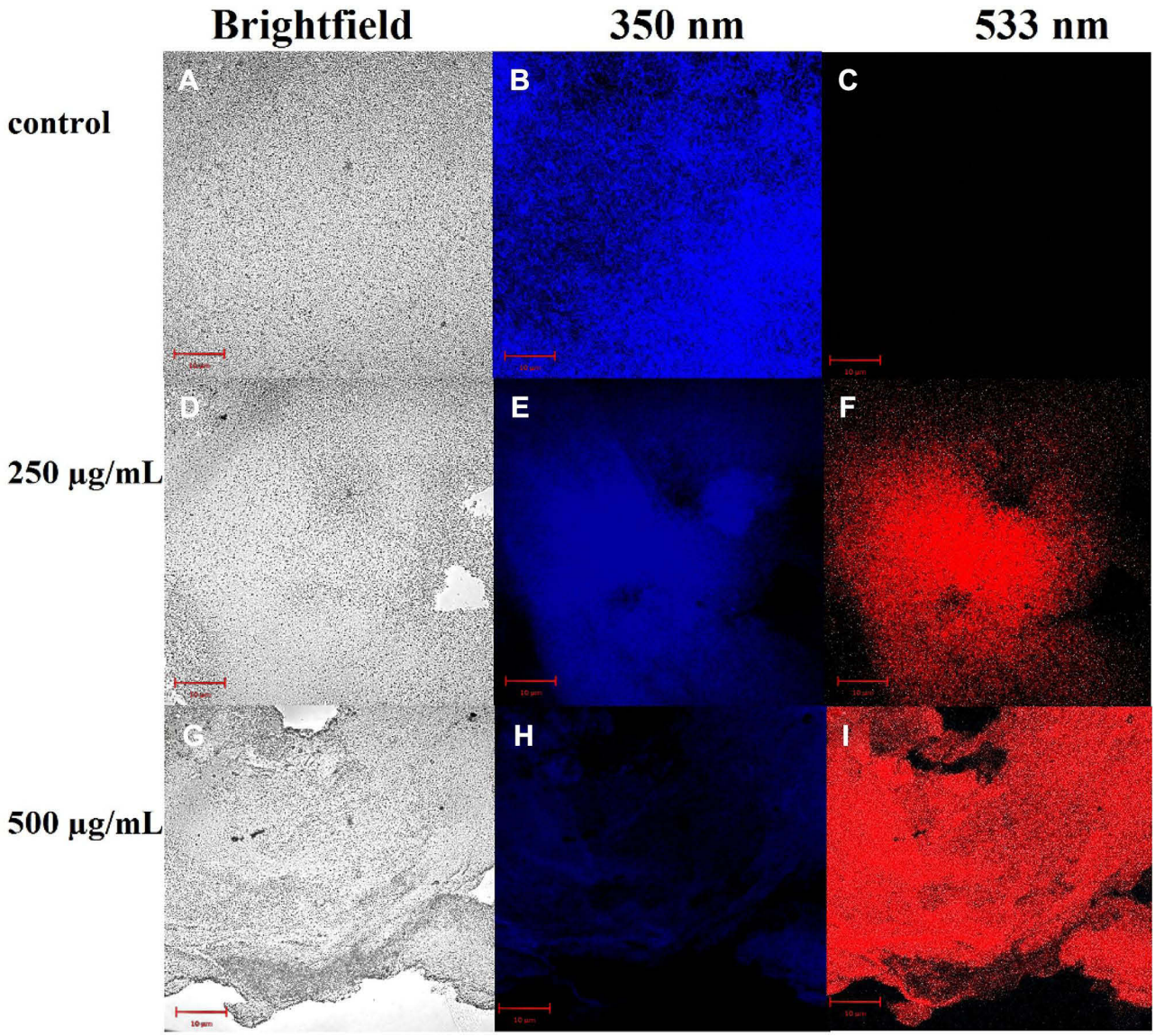

Figure 5 Confocal fluorescence image for *S. aureus* biofilm dyed in PI/DAPI exhibiting the existence of live bacteria (blue) and dead bacteria (red) upon treatment using (**A-C**) PBS, (**D-F**) 250 μg/mL QCS-EDA-CDs and (**G-I**) 500 μg/mL QCS-EDA-CDs for 2.5 h.

EDA-CDs exhibits stronger inhibitory ability against biofilm, in accordance to the dying results of QCS-EDA-CDs, and further proving the potential application of QCS-EDA-CDs as effective antibacterial agent in eliminating biofilms.

Antibacterial Mechanism of QCS-EDA-CDs

The antibacterial mechanism of QCS-EDA-CDs is explored with *S. aureus* as the model bacteria. As shown in SEM images (Figure 6A), the mature bacterial biofilm shows aggregation of complete cells connected and coated with EPS, and the bacterial cells are full. After being treated by QCS-EDA-CDs for four hours, the biofilm shows obvious decrease in its density, and the decrease in bacteria amount (Figure 6B). The bacterial cells are wrinkled, and the surface are seriously damaged and collapsed. The wrinkled and collapsed shape of bacteria prove the disruption of membrane integrity induced by QCS-EDA-CDs, while in control group, bacteria in normal cultivation condition have a spherical structure. The result shows that QCS-EDA-CDs kill bacteria mainly through rupturing its cell membranes.

The prepared QCS-EDA-CDs have been proven to possess excellent antibacterial capacity towards Gram-positive and negative bacteria. Considering the crucial role of QCS-EDA-CDs' surface-chemical properties in interaction activity

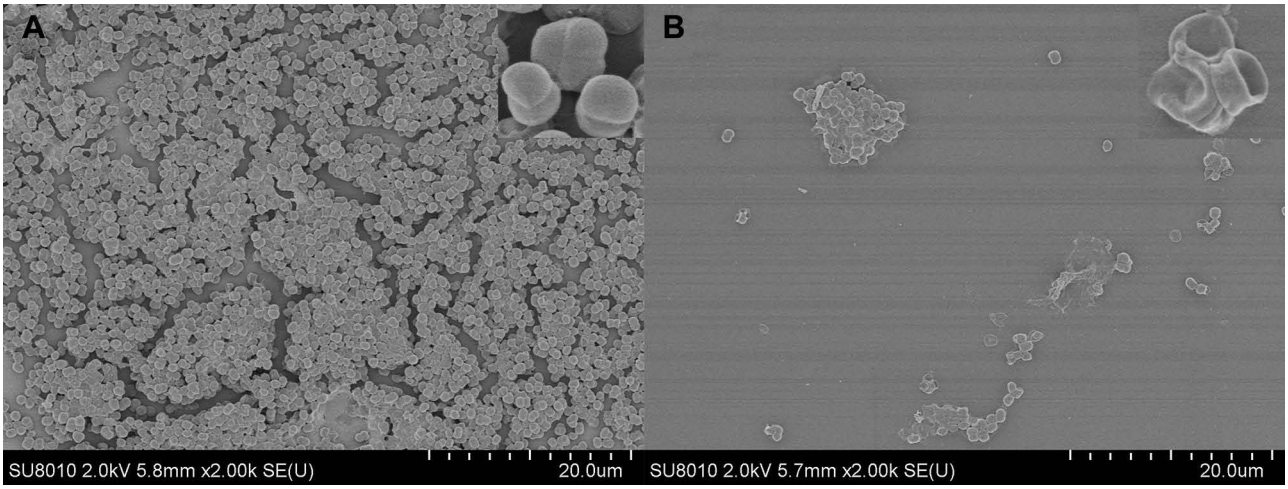

Figure 6 SEM images of *S. aureus* biofilm incubated for 4 h upon treatment of (**A**) PBS and (**B**) QCS-EDA-CDs (800 μg/mL), respectively.

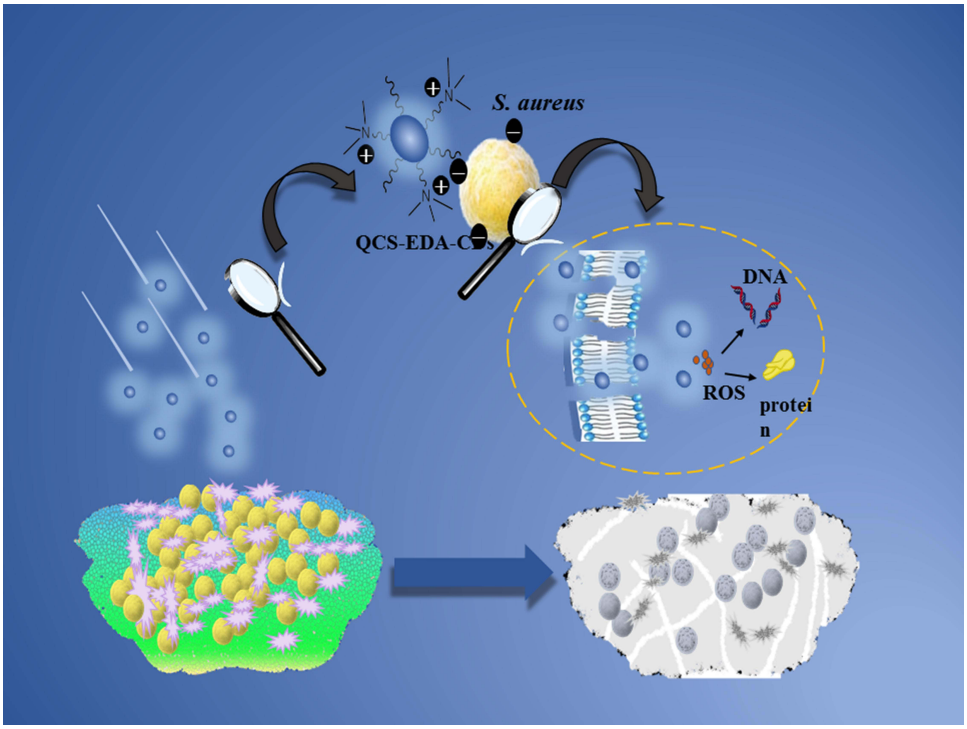

Scheme 2 Schematic diagram exhibiting QCS-EDA-CDs' attack against *S. aureus*. QCS-EDA-CDs attach to the cell membrane by charge interactions, thus piercing cell membrane and damaging the DNA and protein of bacterial cells.

have been studied through calculating their charges, QCS-EDA-CDs are reported to have positive charges (ca. +20.6 mV), while bacterial cell surface have negative charges. Former researches revealed positive charge's conducive role in increasing membrane permeability and final damage to bacterial membrane.[46] It is concluded that QCS-EDA-CDs realize the antibacterial activity through destroying the cell membrane and decomposing EPS. The small size and the hydrophobic organic chain of QCS-EDA-CDs make them easy to enter the substrate layer of biofilm, and the rich quaternary ammonium cations on the surface of CDs would interact with biofilm, destroying the matrix structure of biofilm and finally destroy the bacterial cells (Scheme 2).

Photodynamic therapy (PDT) belongs to a conventional therapy against bacteria. With oxygen, photosensitizer transfers absorbed photon energy to oxygen molecules nearby, and generates reactive oxygen species (ROS) with $^1O_2$

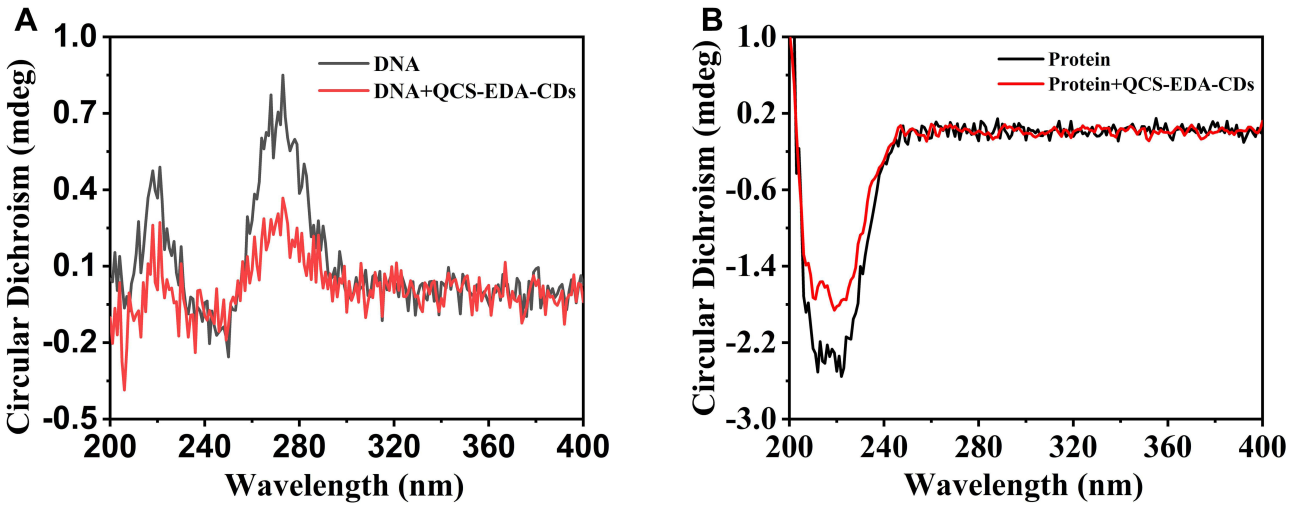

Figure 7 (**A**) Circular dichroism spectra for DNA with and without QCS-EDA-CDs treatment. (**B**) Circular dichroism spectra for *S. aureus* protein with and without QCS-EDA-CDs.

or free radicals, causing the death of bacteria and tissue damage. The fluorescence from the photosensitizer under light activation can be used in disease positioning, light diagnosis and molecule imaging.[47] SOSG has interactions with $^1O_2$ to generate SOSG endoperoxides (SOSG-EP) and releases intense green fluorescence at the maximum intensity of 540 nm.[48] The daylight lamp could be used as the light source. As shown in Figure S5, in contrast to pure SOSG (2.5 μM) group, the solution added with the presence of QCS-EDA-CDs exhibit obviously stronger fluorescence intensity, showing the formation of $^1O_2$. The pure QCS-EDA-CDs do not exhibit any fluorescence at 540 nm after the illumination of 30 min, illustrating that the fluorescence intensity change originates from the combination of SOSG and reactive oxygen species.

Circular dichroism spectroscopy can be considered a meaningful approach to detect the secondary structure for DNA and proteins in the solution.[49] It was used to examine the impact of QCS-EDA-CDs on DNA. As shown in Figure 7A, in comparison with the control group, the decline of QCS-EDA-CDs group's peak suggests that QCS-EDA-CDs loosen DNA's double helix structure. Because of the nanoscale size, QCS-EDA-CDs penetrate into the bacterial cell upon penetrating the cell membrane, and loosen the naked DNA structure of bacteria, thus hindering the proliferation of bacteria. Total protein of *S. aureus* is retrieved using the bacterial total protein extraction kit, and circular dichroism spectroscopy is applied in the study on the interaction of QCS-EDA-CDs with the total protein of *S. aureus*. Without the presence of QCS-EDA-CDs, there exists a broad absorption peak at about 220 nm as the result of the n→π* transition in the α-helical structure (Figure 7B).[50] After the incubation with QCS-EDA-CDs, the weakened CD signal proves the reduced α-helical structure of protein because of the interaction between CDs and protein, leading to the change in hydrogen bond network and secondary structures of proteins, and consequently the damages of bacteria activities. Upon protein incubation with QCS-EDA-CDs, three new protein absorption peaks are found at 202 and 203 nm, suggesting the presence of QCS-EDA-CDs influences protein structural characteristics. The experimental results verify the antibacterial activity of QCS-EDA-CDs is through changing the protein and DNA structure for bacteria.

Alternatively, as shown in Scheme 2, QCS-EDA-CDs damage cell membranes, intracellular protein and DNA, eventually resulting in bacterial death to exert antimicrobial effects. Admittedly, for better understanding the specific targets and detailed mechanism of QCS-EDA-CDs for bacteria, other related experiments and technologies should be also verified, such as the investigation on the anti-quorum sensing activity of CDs as fungal crude extracts,[51] to adjust the biofilm formation.

Biocompatibility Assay of QCS-EDA-CDs

Cytotoxicity is regarded as one of the important factors that determine the safety of biomedical materials, and the cytotoxicity and blood compatibility of QCS-EDA-CDs in the cell are therefore detected. LO2 cells are used as the target

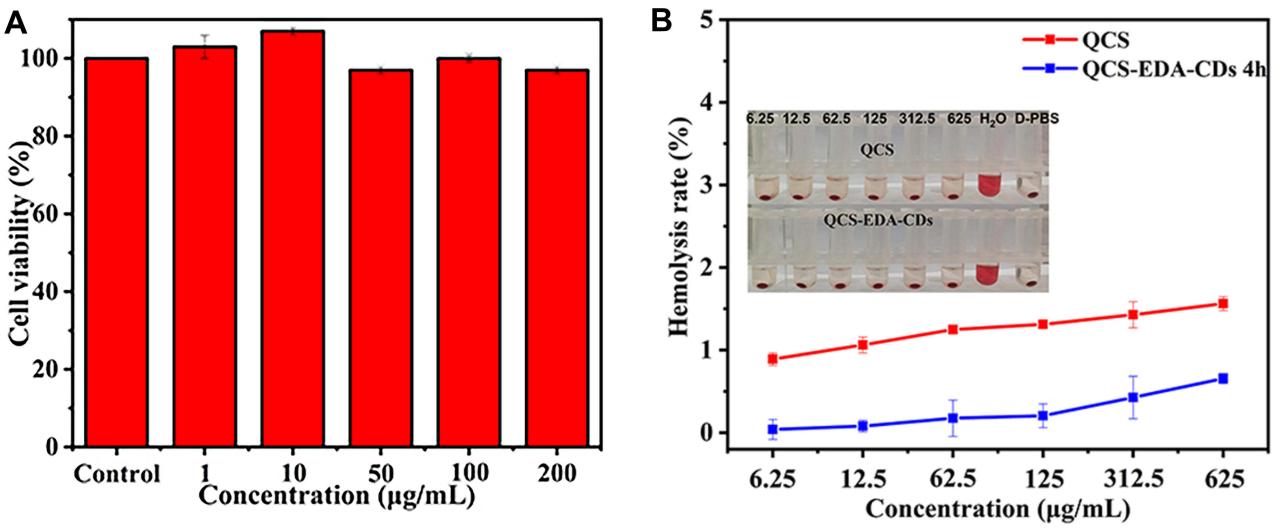

Figure 8 (**A**) Cell viability in LO2 cells at different QCS-EDA-CDs concentrations with DMSO as the positive control. (**B**) Hemolysis rate of QCS-EDA-CDs at different concentrations. Data are mean (SD ± n = 3).

bacteria to test the in vitro cytotoxicity of QCS-EDA-CDs. Figure 8A shows the proliferation rates of cells cultured at different doses of QCS-EDA-CDs in 48 h. MTT assay reveals that average cell viability exceeds 97% when QCS-EDA-CDs concentration is at 200 μg/mL. The finding promotes QCS-EDA-CDs as ideal candidates to use in cellular imaging for diagnosis purposes.

Moreover, an in vitro hemolysis assay is conducted on defibrinated human blood to explain the biocompatibility of QCS-EDA-CDs and QCS of red blood cells (RBCs) in biological solution. Spectrophotometric analysis on supernatants and photographs for treated RBCs are gathered after exposing RBCs to QCS-EDA-CDs and QCS at different concentrations in 3 h (Figure 8B). Notably, the supernatant in the RBC suspension remains clear, with a measured concentration of 500 μg/mL. When the sample concentration exceeds 500 μg /mL, the hemolysis rates in QCS-EDA-CDs and QCS are less than 0.08% and 1.06%. A hemolysis rate below 5% is secure in biomedical applications. This result indicates that QCS-EDA-CDs do not lead to the rupture and hemolysis in red blood cells in physiological conditions and shows excellent blood compatibility.

Conclusion

In summary, with CS and its derivatives as raw materials, a variety of blue-fluorescent CDs are prepared through simple and fast one-step hydrothermal route, to study how carbon source affected CDs in optical properties and antibacterial activities. Through carefully selecting proper raw material type and synthesis parameters, QCS-EDA-CDs with high antibacterial ability are prepared. Numerous characterization means are adopted to examine the antibacterial mechanism and process of QCS-EDA-CDs against bacteria. The experiments show that the rich quaternary ammonium groups on QCS-EDA-CDs make CDs strong positively charged, leading to easy combination with the negative charges on the surface of bacterial cells. QCS-EDA-CDs could destroy the protein and the secondary structure of DNA, cause the disorder of normal functions, and finally kill bacterial cells. Meanwhile, QCS-EDA-CDs have been proven to induce single oxygen under daylight lamp and could realize antibacterial effect through multiple mechanisms. The prepared CDs could also inhibit the growth of biofilm of *S. aureus*. Due to their excitation wavelength dependency property, QCS-EDA-CDs have been applied in the imaging of bacterial cells and biofilm. Cytotoxicity and hemolysis tests also show their excellent biocompatibility. These results show the potential application values of QCS-EDA-CDs in novel fluorescence labeling, biomedical imaging and visual treatment of bacterial infection.

Acknowledgments

This work was funded by the National Natural Science Foundation of China (21978329) and the Fundamental Research Funds for Central Universities of South-central University for Nationalities (CZY19029, CZP20004).

Disclosure

The authors report no conflicts of interest in this work.

References

1. Yougbare S, Chou HL, Yang CH, et al. Facet-dependent gold nanocrystals for effective photothermal killing of bacteria. *J Hazard Mater*. 2021;407:124617. doi:10.1016/j.jhazmat.2020.124617
2. Parasuraman P, Shaji C, Sharan A. Biogenic Silver Nanoparticles Decorated with Methylene Blue Potentiated the Photodynamic Inactivation of Pseudomonas aeruginosa and Staphylococcus aureus. *Pharmaceutics*. 2020;12(8):709. doi:10.3390/pharmaceutics12080709
3. Parasuraman P, Anju VT, Lal SBS, et al. Synthesis and antimicrobial photodynamic effect of methylene blue conjugated carbon nanotubes on E. coli and S. aureus. *Photochem Photobiol Sci*. 2019;18(2):563–576. doi:10.1039/c8pp00369f
4. Anju VT, Paramanantham P, Siddhardha B, et al. Malachite green-conjugated multi-walled carbon nanotubes potentiate antimicrobial photodynamic inactivation of planktonic cells and biofilms of Pseudomonas aeruginosa and Staphylococcus aureus. *Int J Nanomed*. 2019;14:3861–3874. doi:10.2147/IJN.S202734
5. Anju VT, Paramanantham P. Antimicrobial photodynamic activity of toluidine blue-carbon nanotube conjugate against Pseudomonas aeruginosa and Staphylococcus aureus - understanding the mechanism of action. *Photodiagnosis Photodyn Ther*. 2019;27:305–316. doi:10.1016/j.pdpdt.2019.06.014
6. Parasuraman P, Antony AP. Antimicrobial photodynamic activity of toluidine blue encapsulated in mesoporous silica nanoparticles against Pseudomonas aeruginosa and Staphylococcus aureus. *Biofouling*. 2019;35(1):89–103. doi:10.1080/08927014.2019.1570501
7. Paramanantham P, Siddhardha B, Lal SBS, et al. Antimicrobial photodynamic therapy on Staphylococcus aureus and Escherichia coli using malachite green encapsulated mesoporous silica nanoparticles: an in vitro study. *PeerJ*. 2019;7:e7454. doi:10.7717/peerj.7454
8. Mutalik C, Krisnawati DI, Patil SB, et al. Phase-Dependent MoS_2 Nanoflowers for Light-Driven Antibacterial Application. *ACS Sustain Chem Eng*. 2021;9(23):7904–7912. doi:10.1021/acssuschemeng.1c01868
9. Feng J, Yu YL, Wang JH. Porphyrin structure carbon dots under red light irradiation for bacterial inactivation. *New J Chem*. 2020;44(42):18225–18232. doi:10.1039/d0nj04013d
10. Li YJ, Harroun SG, Su YC, et al. Synthesis of self-assembled spermidine-carbon quantum dots effective against multidrug-resistant bacteria. *Adv Healthc Mater*. 2016;5(19):2545–2554. doi:10.1002/adhm.201600297
11. Bing W, Sun H, Yan Z, Ren J, Qu X. Programmed bacteria death induced by carbon dots with different surface charge. *Small*. 2016;12(34):4713–4718. doi:10.1002/smll.201600294
12. Li H, Huang J, Song Y, et al. Degradable carbon dots with broad-spectrum antibacterial activity. *ACS Appl Mater Interfaces*. 2018;10(32):26936–26946. doi:10.1021/acsami.8b08832
13. Mutalik C, Okoro G, Krisnawati DI, et al. Copper sulfide with morphology-dependent photodynamic and photothermal antibacterial activities. *J Colloid Interface Sci*. 2022;607:1825–1835. doi:10.1016/j.jcis.2021.10.019
14. Siddhardha B, Pandey U, Kaviyarasu K, et al. Chrysin-Loaded Chitosan Nanoparticles Potentiates Antibiofilm Activity against Staphylococcus Aureus. *Pathogens*. 2020;9(2):115. doi:10.3390/pathogens9020115
15. Liang G, Shi H, Qi Y, et al. Specific Anti-biofilm Activity of Carbon Quantum Dots by Destroying P. gingivalis Biofilm Related Genes. *Int J Nanomed*. 2020;15:5473–5489. doi:10.2147/IJN.S253416
16. Li P, Liu S, Zhang G, et al. Design of pH-responsive dissociable nanosystem based on carbon dots with enhanced anti-biofilm property and excellent biocompatibility. *ACS Appl Bio Mater*. 2020;3(2):1105–1115. doi:10.1021/acsabm.9b01053
17. Singh AK, Prakash P, Singh R, et al. Curcumin quantum dots mediated degradation of bacterial biofilms. *Front Microbiol*. 2017;8:1517. doi:10.3389/fmicb.2017.01517
18. Wang K, Ji Q, Li H, et al. Synthesis and antibacterial activity of silver@carbon nanocomposites. *J Inorg Biochem*. 2017;166:64–67. doi:10.1016/j.jinorgbio.2016.11.002
19. Song Y, Lu F, Li H, et al. Degradable carbon dots from cigarette smoking with broad-spectrum antimicrobial activities against drug-resistant bacteria. *ACS Appl Bio Mater*. 2018;1(6):1871–1879. doi:10.1021/acsabm.8b00421
20. Li X, Yeh YC, Giri K, et al. Control of Nanoparticle Penetration into Biofilms through Surface Design. *Chem Commun*. 2015;51:282–285. doi:10.1039/C4CC07737G
21. Chen S, Li Q, Wang X, Yang YW, Gao H. Multifunctional bacterial imaging and therapy systems. *J Mater Chem B*. 2018;6(32):5198–5214. doi:10.1039/C8TB01519H
22. Travlou NA, Giannakoudakis DA, Algarra M, Labella AM, Rodríguez-Castellón E, Bandosz TJ. N-doped carbon quantum dots: surface chemistry dependent antibacterial activity. *Carbon*. 2018;135:104–111. doi:10.1016/j.carbon.2018.04.018
23. Jian HJ, Wu RS, Lin TY, et al. Super-cationic carbon quantum dots synthesized from spermidine as an eye drop formulation for topical treatment of bacterial keratitis. *ACS Nano*. 2017;11(7):6703–6716. doi:10.1021/acsnano.7b01023
24. Cui F, Ye Y, Ping J, Sun X. Carbon dots: current advances in pathogenic bacteria monitoring and prospect applications. *Biosens Bioelectron*. 2020;156:112085. doi:10.1016/j.bios.2020.112085
25. Huang P, Lin J, Wang X, et al. Light-triggered theranostics based on photosensitizer-conjugated carbon dots for simultaneous enhanced-fluorescence imaging and photodynamic therapy. *Adv Mater*. 2012;24(37):5104–5110. doi:10.1002/adma.201200650
26. Li H, Kang Z, Liu Y, Lee ST. Carbon nanodots: synthesis, properties and applications. *J Mater Chem*. 2012;22(46):24230–24253. doi:10.1039/C2JM34690G

27. Niu WJ, Li Y, Zhu R, Shan D, Fan YR, Zhang XJ. Ethylenediamine-assisted hydrothermal synthesis of nitrogen-doped carbon quantum dots as fluorescent probes for sensitive biosensing and bioimaging. *Sens Actuators B*. 2015;218:229–236. doi:10.1016/j.snb.2015.05.006
28. Sun S, Zhang L, Jiang K, Wu A, Lin H. Toward high-efficient red emissive carbon dots: facile preparation, unique properties, and applications as multifunctional theranostic agents. *Chem Mater*. 2016;28(23):8659–8668. doi:10.1021/acs.chemmater.6b03695
29. Vishwakarma S, Rajani M, Bagul M, Goyal R. A rapid method for the isolation of swertiamarin from Enicostemma littorale. *Pharm Biol*. 2004;42 (6):400–403. doi:10.1080/13880200490885095
30. Ding H, Wei JS, Zhang P, Zhou ZY, Gao QY, Xiong HM. Solvent-controlled synthesis of highly luminescent carbon dots with a wide color gamut and narrowed emission peak widths. *Small*. 2018;14(22):1800612. doi:10.1002/smll.201800612
31. Wang Y, Hu A. Carbon quantum dots: synthesis, properties and applications. *J Mater Chem C*. 2014;2:6921–6939. doi:10.1039/C4TC00988F
32. Wang H, Zhang M, Ma Y, et al. Selective inactivation of Gram-negative bacteria by carbon dots derived from natural biomass: Artemisia argyi leaves. *J Mater Chem B*. 2020;8(13):2666–2672. doi:10.1039/C9TB02735A
33. Datta KKR, Qi G, Zboril R, Giannelis EP. Yellow emitting carbon dots with superior colloidal, thermal, and photochemical stabilities. *J Mater Chem C*. 2016;4(41):9798–9803. doi:10.1039/C6TC03452G
34. Jiang K, Wang Y, Gao X, Cai C, Lin H. Facile, quick, and gram-scale synthesis of ultralong-lifetime room-temperature-phosphorescent carbon dots by microwave irradiation. *Angew Chem Int Edit*. 2018;57(21):6216–6220. doi:10.1002/anie.201802441
35. Chen F, Shi Z, Neoh KG, Kang ET. Antioxidant and antibacterial activities of eugenol and carvacrol-grafted chitosan nanoparticles. *Biotechnol Bioeng*. 2009;104(1):30–39. doi:10.1002/bit.22363
36. Zhao C, Wu L, Wang X, et al. Quaternary ammonium modified carbon quantum dots as an antimicrobial agent against gram-positive bacteria for the treatment of MRSA-infected pneumonia in mice. *Carbon*. 2020;163:70–84. doi:10.1016/j.carbon.2020.03.009
37. Yang J, Zhang X, Ma Y, et al. Carbon dot-based platform for simultaneous bacterial distinguishment and antibacterial applications. *ACS Appl Mater Interfaces*. 2016;8(47):32170–32181. doi:10.1021/acsami.6b10398
38. Yuan H, Liu Z, Liu L, Lv F, Wang Y, Wang S. Cationic conjugated polymers for discrimination of microbial pathogens. *Adv Mater*. 2014;26:4333–4338. doi:10.1002/adma.201400636
39. Forster BM, Marquis H. Protein transport across the cell wall of monoderm gram-positive bacteria. *Mol Microbiol*. 2012;84:405–413. doi:10.1111/j.1365-2958.2012.08040.x
40. Lu F, Ma Y, Wang H, et al. Water-solvable carbon dots derived from curcumin and citric acid with enhanced broad-spectrum antibacterial and antibiofilm activity. *Mater Today Commun*. 2021;26:102000. doi:10.1016/j.mtcomm.2020.102000
41. Lin F, Li C, Chen Z. Bacteria-derived carbon dots inhibit biofilm formation of Escherichia coli without affecting cell growth. *Front Microbiol*. 2018;9:259. doi:10.3389/fmicb.2018.00259
42. Ran HH, Cheng X, Bao YW, et al. Multifunctional quaternized carbon dots with enhanced biofilm penetration and eradication efficiencies. *J Mater Chem B*. 2019;7(33):5104–5114. doi:10.1039/C9TB00681H
43. Li P, Yang X, Zhang X, et al. Surface chemistry-dependent antibacterial and antibiofilm activities of polyamine-functionalized carbon quantum dots. *J Mater Sci*. 2020;55(35):16744–16757. doi:10.1007/s10853-020-05262-6
44. Li X, Huang R, Tang FK, et al. Red-Emissive Guanylated Polyene-Functionalized Carbon Dots Arm Oral Epithelia against Invasive Fungal Infections. *ACS Appl Mater Interfaces*. 2019;11(50):46591–46603. doi:10.1021/acsami.9b18003
45. Carlson RP, Taffs R, Davison WM, Stewart PS. Anti-biofilm properties of chitosan-coated surfaces. *J Biomater Sci Polymer*. 2008;19 (8):1035–1046. doi:10.1163/156856208784909372
46. Ju B, Nie H, Zhang XG, et al. Inorganic salt incorporated solvothermal synthesis of multicolor carbon dots, emission mechanism, and antibacterial study. *ACS Appl Nano Mater*. 2018;1(11):6131–6138. doi:10.1021/acsanm.8b01355
47. Nie X, Jiang C, Wu S, et al. Carbon quantum dots: a bright future as photosensitizers for in vitro antibacterial photodynamic inactivation. *J Photochem Photobiol*. 2020;206:111864. doi:10.1016/j.jphotobiol.2020.111864
48. Lin H, Shen Y, Chen D, et al. Feasibility study on quantitative measurements of singlet oxygen generation using singlet oxygen sensor green. *J Fluoresc*. 2013;23(1):41–47. doi:10.1007/s10895-012-1114-5
49. Baase WA, Johnson J. Circular dichroism and DNA secondary structure. *Nuc Acids Res*. 1979;6(2):797–814. doi:10.1093/nar/6.2.797
50. Kelly SM, Jess TJ, Price NC. How to study proteins by circular dichroism, *Biochim. Biophys Acta*. 2005;1751:119–139. doi:10.1016/j.bbapap.2005.06.005
51. Pattnaik SS, Ranganathan SK, Ampasala DR, Syed A, Ameen F, Busi S. Attenuation of quorum sensing regulated virulence and biofilm development in Pseudomonas aeruginosa PAO1 by Diaporthe phaseolorum SSP12. *Microb Pathog*. 2018;118:177–189. doi:10.1016/j.micpath.2018.03.031